Stem Cell Research & Therapy

RESEARCH

Open Access

Multiomics analyses reveal adipose-derived stem cells inhibit the inflammatory response of M1-like macrophages through secreting lactate

Tetsuhiro Horie[1,2], Hiroaki Hirata[3*], Takuya Sakamoto[1,2], Hironori Kitajima[3], Atsushi Fuku[3], Yuka Nakamura[1], Yumi Sunatani[4], Ikuhiro Tanida[5], Hiroshi Sunami[6], Yoshiyuki Tachi[3], Yasuhito Ishigaki[1], Naoki Yamamoto[7], Yusuke Shimizu[8], Toru Ichiseki[3*], Ayumi Kaneuji[3], Kuniyoshi Iwabuchi[4], Satoshi Osawa[5] and Norio Kawahara[3]

Abstract

Background Adipose-derived stem cells (ADSCs) are widely used in the field of regenerative medicine because of their various functions, including anti-inflammatory effects. ADSCs are considered to exert their anti-inflammatory effects by secreting anti-inflammatory cytokines and extracellular vesicles. Although recent studies have reported that metabolites have a variety of physiological activities, whether those secreted by ADSCs have anti-inflammatory properties remains unclear. Here, we performed multiomics analyses to examine the effect of ADSC-derived metabolites on M1-like macrophages, which play an important role in inflammatory responses.

Methods The concentration of metabolites in the culture supernatant of ADSCs was quantified using capillary electrophoresis time-of-flight mass spectrometry. To evaluate their effects on inflammatory responses, M1-like macrophages were exposed to the conditioned ADSC medium or their metabolites, and RNA sequencing was used to detect gene expression changes. Immunoblotting was performed to examine how the metabolite suppresses inflammatory processes. To clarify the contribution of the metabolite in the conditioned medium to its anti-inflammatory effects, metabolite uptake was pharmacologically inhibited, and gene expression and the tumor necrosis factor-α concentration were measured by quantitative PCR and enzyme-linked immunosorbent assay, respectively.

Results Metabolomic analysis showed large amounts of lactate in the culture supernatant. The conditioned medium and lactate significantly suppressed or increased the pro-inflammatory and anti-inflammatory gene expressions. However, sequencing and immunoblotting analysis revealed that lactate did not induce polarization from M1- to M2-like macrophages. Based on a recent report that the immunosuppressive effect of lactate depends on epigenetic reprogramming, histone acetylation was investigated, and H3K27ac expression was upregulated. In addition, 7ACC2, which specifically inhibits the monocarboxylate transporter 1, significantly inhibited the anti-inflammatory effect of the conditioned ADSC medium on M1-like macrophages.

*Correspondence:
Hiroaki Hirata
hiro6246@kanazawa-med.ac.jp
Toru Ichiseki
tsy-ichi@kanazawa-med.ac.jp
Full list of author information is available at the end of the article

Conclusions Our results showed that ADSCs suppress pro-inflammatory effects of M1-like macrophages by secreting lactate. This study adds to our understanding of the importance of metabolites and is also expected to elucidate new mechanisms of ADSC treatments.

Keywords Adipose-derived stem cell, Lactate, Macrophage, Metabolomics, Transcriptomics, Bioinformatics

Background

In recent years, regenerative medicine using stem cells has become a new treatment strategy [1–4]. Cell therapy can not only alleviate symptoms, but also regenerate tissues, something difficult to accomplish with existing methods. Recently, induced pluripotent stem cells (iPSCs) have been used for regenerative medicine [5]. Already some clinical trials have used iPSCs to regenerate organs (e.g., cardiac muscle and retina), and iPSCs are expected to revolutionize regenerative medicine [6, 7]. However, there are issues to be resolved before iPSCs can be used for clinical applications, such as the risk of tumorigenicity, immunogenicity, financial cost, and unestablished methods of differentiation into the desired cells [8, 9]. On the other hand, adult stem cells like hematopoietic stem cells and neural stem cells, which exist in vivo, have similar properties to iPSCs [10–12]. While having a more limited ability to differentiate than iPSCs, they are more convenient and safer and have been already used clinically, for example, in the treatment of acute myeloid leukemia [13, 14]. Among adult stem cells, mesenchymal stem/stromal cells (MSCs) are particularly promising for clinical applications [15].

MSCs can differentiate into at least three lineages (osteoblasts, chondrocytes and adipocytes) in vitro, being widely distributed throughout the body, including the bone marrow, umbilical cord, placenta and dental pulp [16, 17]. Among them, adipose-derived stem cells (ADSCs), abundant in the adipose tissue, can be harvested with minimal invasiveness by liposuction and have high proliferative potential [18, 19]. MSCs/ADSCs have immunomodulatory effects, which explain their use as treatments for various diseases associated with inflammation like graft-versus-host disease, rheumatoid arthritis, and osteoarthritis (OA) [20, 21]. Previous studies showed that the therapeutic effect of MSCs/ADSCs in these diseases is related to their anti-inflammatory properties, mediated by cytokines such as IL-10 and extracellular vesicles (EVs) [22, 23]. Indeed, these molecules suppress inflammation by polarizing inflammatory M1-like macrophages into anti-inflammatory M2-like macrophages in vitro and in vivo [24–26]. Nuclear factor-kappa B (NF-κB) signaling plays a central role in macrophage activation; these anti-inflammatory molecules have been reported to suppress inflammation partly by reducing the production of inflammatory cytokines like tumor necrosis factor-alpha (TNF-α) by suppressing of NF-κB signaling [27, 28]. Thus, a potential way to enhance the therapeutic effect is to administer cytokines/EVs together with ADSCs; however, it is costly and technically difficult to prepare high-quality cytokines and EVs, and their safety has not been determined yet.

Recent studies revealed a close relationship between macrophage function and intracellular energy metabolism. For instance, lipopolysaccharide (LPS) stimulation of M1-like macrophages increases glucose uptake and enhances the glycolytic system, while inhibition of that system suppresses pro-inflammatory response [29, 30]. Interestingly, these changes have been reported to involve epigenetics, i.e., gene expression regulation. Epigenetic reprogramming includes DNA methylation and histone modifications, which regulate gene expression over long periods. In particular, histones are acetylated by histone acetyltransferase, which loosens the nucleosome structure and enhances gene expression [31, 32]. Noe et al. have shown that histone acetylation contributes to interleukin (IL)−4-induced M2-like macrophage polarization [33]. Furthermore, Shi et al. [34] most recently reported that lactate (LA) exhibits anti-inflammatory effects by suppressing the transcription of pro-inflammatory-related genes via H3K27 acetylation rather than by inducing polarization toward M2-like macrophages or suppressing NF-κB signaling.

Metabolites exhibit various physiological activities; for example, the inosine secreted by brown adipocytes stimulates energy expenditure [35]. In addition, certain metabolite combinations derived from apoptotic cells ameliorate inflammation [36]. However, the anti-inflammatory effects of ADSC-derived metabolites remain unknown. This study aimed to identify a novel mechanism of immunosuppressive properties of ADSCs by performing metabolomic and transcriptomic analyses and revealed that they suppress inflammation through LA secretion, which is partially mediated by the monocarboxylate transporter and H3K27 acetylation.

Methods

Cell culture

In this study, we used human ADSCs derived from six healthy donors who provided informed consent or were purchased from Lonza (Cat. #PT-5006). Details about the donors are shown in Supplementary Table 1. ADSCs

were isolated according to a previous report [37], being cultured in KBM ADSC-1 or KBM ADSC-4 (Kohjin Bio) and expanded within seven passages. Human monocytic THP-1 cells (RIKEN BRC) were cultured in Roswell Park Memorial Institute 1640 (RPMI-1640) supplemented with 10% heat-inactivated fetal bovine serum (FBS) and 1% penicillin/streptomycin at 37℃ in 5% CO_2. THP-1 cells were differentiated with 100 ng/mL of phorbol 12-myristate 13-acetate (PMA, FUJIFILM Wako Pure Chemicals) treatment for 24 h. Then, the medium was changed, and cells were polarized toward M1-like macrophages by 24-h exposure to 100 ng/mL of LPS (Sigma-Aldrich).

Metabolome analysis

ADSCs donated by healthy people were cultured in KBM ADSC-4 until approximately 70% confluency; then the conditioned medium (CM) was harvested and transported to Human Metabolome Technologies, Inc. (Yamagata, Japan). A mixture of 80 µL of the CM plus 20 µL of aqueous solution containing internal controls was ultrafiltrated, and the filtrate was used for capillary electrophoresis time-of-flight mass spectrometry (CE-TOFMS). CE-TOFMS analysis of cationic and anionic metabolites was performed using an Agilent CE-TOFMS system (Agilent Technologies). Signal peaks with a signal-to-noise ratio > 3 were extracted by MasterHands (Keio University); detected peaks were annotated for all substances registered in the HMT metabolite library based on the *m/z* and migration time, allowing an error of ± 10 ppm and ± 0.5 min, respectively. Mass spectrometry data was provided as Additional File 2.

Z-score calculation and heatmap creation were performed using the genefilter and pheatmap R packages, respectively. Samples were hierarchically clustered using the "ward.D2" method. Principal component analysis (PCA) was carried out using "prcomp" function and plotted with the ggbiplot R package. Metabolite set enrichment analysis (MSEA) was conducted using MetaboAnalyst 5.0 (https://genap.metaboanalyst.ca/MetaboAnalyst/); a false discovery rate (FDR) < 0.1 was considered significant.

Flow cytometry

Cultured cells were washed with phosphate buffered saline (PBS) and trypsinized. Detached cells were suspended in Cell Staining Buffer (BioLegend) containing Human TruStain FcX (BioLegend) for Fc receptor blocking, followed by incubation with a cocktail of antibodies. Then, the stained cells were re-suspended in Cell Staining Buffer and analyzed using BD FACSCanto II (BD Biosciences). To detect apoptotic cells, Fc-blocked cells were washed with Cell Staining Buffer and re-suspended in Annexin V Binding Buffer (BioLegend) containing 7-aminoactinomycin D (7-AAD) and an anti-Annexin V antibody. In this study, Annexin V^+ 7-AAD^- cells were defined as apoptotic cells. Details on antibodies are included in Supplementary Table 2.

Preparation of CM

ADSCs suspended in KBM ADSC-1 were seeded into 10 cm dishes and cultured until cells reached 70% confluency. Then, the medium was changed to RPMI-1640/10% heat-inactivated FBS and cultured for 72 h. Next, the CM was harvested, centrifuged, and stored at − 80 °C. The LA concentration of the CM was measured using the Lactate Assay Kit-WST (DOJINDO) following the manufacturer's instructions. The LA concentration in the CM of commercially available and freshly isolated ("in-house") ADSCs used in the experiments is shown in Fig. S1.

RNA sequencing (RNA-seq)

Total RNA extraction and DNase I treatment were performed using an RNeasy Mini Kit and RNase-Free DNase Set (QIAGEN), respectively. RNA integrity was determined using a 2100 Bioanalyzer and RNA 6000 Nano Kit (Agilent Technologies); all samples having an RNA Integrity Number > 9 were sent to Bioengineering Lab. Co., Ltd. (Kanagawa, Japan). Following quality check using a 5200 Fragment Analyzer System and Agilent HS RNA Kit (Agilent Technologies), DNA libraries were prepared using MGIEasy RNA Directional Library Prep Set (MGI Tech); the quality of the libraries was investigated using a 5200 Fragment Analyzer System and dsDNA 915 Reagent Kit (Agilent Technologies). The libraries were then circularized and prepared as DNA Nanoball using a MGIEasy Circularization Kit and a DNBSEQ-G400RS High-throughput Sequencing Kit (MGI Tech), respectively. Sequencing was performed on the DNBSEQ-G400 sequencer (MGI Tech) (2 × 100 bp).

The quality of sequencing data was checked using FastQC (ver. 0.12.1). Adaptor sequences and low-quality reads (quality score < 30, read length < 30, N > 5) were trimmed using fastp (ver. 0.23.3). Then, clean reads were aligned to the human reference sequence (GRCh38.p13) using STAR (ver. 2.7.10b), and gene counts and transcripts per million (TPM) values were calculated using RSEM (ver. 1.3.1). Differentially expressed genes were determined using a likelihood ratio test with the edgeR R package ("glmLRT" function). PCA was performed as described above. Volcano plots and Venn diagrams were drawn using the EnhancedVolcano and VennDiagram R packages, respectively. Gene ontology (GO) analysis was carried out using the clusterProfiler R package.

Quantitative polymerase chain reaction (qPCR)

Total RNA was extracted as described above, followed by cDNA synthesis using SuperScript III First-Strand Synthesis System (Thermo Fisher Scientific) with oligo(dT) primers. qPCR was performed using a KAPA SYBR Fast qPCR Kit (Kapa Biosystems) on the QuantStudio 12 K Flex Real-Time PCR System (Thermo Fisher Scientific). *GAPDH* was used as loading control. Sequences of gene-specific primers are listed in Supplementary Table 3.

Immunoblotting

Cells were washed with ice-cold PBS and then lysed in RIPA buffer (Thermo Fisher Scientific) containing protease inhibitor cocktail (Roche). Cell lysates treated with Sample Buffer Solution (FUJIFILM Wako Pure Chemicals) were subjected to SDS-PAGE and transferred to PVDF membranes (Millipore). Membranes were blocked with EveryBlot Blocking Buffer (Bio-rad) for 5 min at room temperature and incubated overnight at 4℃ with a primary antibody diluted in the buffer. The next day, membranes were washed with tris-buffered saline with Tween 20 (TBS-T) and incubated for 1 h at room temperature with a secondary antibody diluted in the buffer. After washing with TBS-T, the blots were developed with ECL Prime Western Blotting Detection Reagents (Cytiva), and chemiluminescence was detected by FUSION FX7 (Vilber Lourmat). Protein levels were quantified using ImageJ software. For fractionating nuclear and cytoplasmic proteins, cells were processed using NE-PER Nuclear and Cytoplasmic Extraction Reagents (Thermo Fisher Scientific) containing protease inhibitor cocktail and phosphatase inhibitor cocktail (Nacalai Tesque). Details about antibodies are given in Supplementary Table 4, and uncropped blots are shown in Additional File 3.

Cell viability assay

THP-1 cells were seeded into a 96-well plate and differentiated/polarized toward M1-like macrophages as described above. Then, medium was replaced with inhibitor-containing medium and incubated for 24 h. Cell viability was determined using Cell Counting Kit-8 (DOJINDO). Dimethyl sulfoxide (DMSO) and 7ACC2 were purchased from Nacalai Tesque and SellekChem, respectively.

To induce apoptosis, ADSCs were treated with p53-MDM2 inhibitor nutlin-3 (SelleckChem). Trypan blue exclusion assay was used with TC20 Automated Cell Counter (Bio-rad) to measure cell viability.

Measuring intracellular lactate concentration

THP-1 cell-derived M1-like macrophages seeded into a 24-well plate were cultured in medium containing 2 μM of 7ACC2 for 1 h, followed by an additional 23 h incubation in medium containing the same concentration of 7ACC2 and 15 mM of LA (Nacalai Tesque). Thereafter, cells were rinsed with ice-cold PBS and lysed using 0.1% Triton-X (Sigma-Aldrich). Cell lysates were centrifuged, and the supernatant was then ultrafiltrated with an Amicon Ultra-0.5 Centrifugal Filter Unit (Merck). The LA concentration in the filtrate was determined using a Lactate Assay Kit-WST. The intracellular LA concentration was calculated by correcting for total protein content as measured using a Protein Assay BCA Kit (Nacalai Tesque).

Enzyme-linked immunosorbent assay (ELISA)

THP-1 cell-derived M1-like macrophages treated with 7ACC2 for 24 h were washed with PBS, before adding fresh medium. After a 4 h incubation, the supernatant was collected, centrifuged, and stored at −80℃ until further use. The concentration of TNF-α contained in the supernatant was quantified using an LBIS Human TNF-α ELISA Kit (FUJIFILM Wako Pure Chemicals).

OA induction

BALB/cSlc-*nu/nu* nude mice were purchased from Japan SLC, Inc. (Shizuoka, Japan). The mice were housed in a specific pathogen-free environment under a 12-h light/dark cycle at 22 ± 2℃ and 40–60% relative humidity, with free access to water and food. Twelve-week-old male mice were randomly divided into four groups, anesthetized with isoflurane, and administered with 2 U/10 μL of type VII collagenase (Sigma-Aldrich) intra-articularly on Days 0 and 2. The same volume of saline was injected as a negative control. Subsequently, on Days 7, 14, 21, and 28, 10 μL of CM from human ADSCs containing DMSO or 7ACC2 (10 μM) was administered intra-articularly. On Day 35, mice were euthanized with CO_2, and tissue was harvested. The work has been reported in line with the ARRIVE guidelines 2.0.

Histology

The tissue was fixed overnight in 10% neutral buffered formalin and decalcified with ethylenediaminetetraacetic acid for one week. Sections were prepared from paraffin-embedded tissue and stained with Safranin O and Fast Green. To evaluate the cartilage damage, the area stained with Safranin O was quantified using Image J (National Institutes of Health). For immunofluorescence staining, deparaffinized sections were blocked using Animal-Free Blocker and Diluent, R.T.U. (Vector Laboratories), and stained with a primary antibody overnight at 4℃. Then, unbound antibodies were washed out with PBS and incubated with a secondary antibody and 4',6-diamidino-2-phenylindole (DAPI) for 1 h at room temperature.

Next, sections were washed using PBS and embedded in ProLong Glass Antifade Mountant (Thermo Fisher Scientific). Capture and analysis were performed using the BZ-X710 fluorescence microscope (Keyence). The antibodies used for histological analysis are listed in Supplementary Table 5. The preparation of the sections and measurements were carried out using different experimenters.

Statistical analysis

Data are represented as mean ± standard deviation. Statistical analysis was performed using R. Except for RNA-seq analysis, comparisons between two groups and among multiple groups were performed using a Student's *t*-test and one- or two-way analysis of variance followed by Dunnett or Tukey–Kramer test, respectively; $P < 0.05$ was considered statistically significant. For RNA-seq analysis, we performed a generalized linear model likelihood ratio test with edgeR and defined statistical significance as FDR < 0.05.

Results

The culture supernatant of ADSCs contains high concentration of lactate

First, we harvested ADSCs from six healthy people and cultured them in serum-free KBM ADSC-4 medium for 24 h before collecting the supernatant. The concentration of metabolites was quantitatively measured using CE-TOFMS; in this study, we analyzed about 1100 water-soluble/ionic metabolites and identified 46. A heatmap showed that the composition of the supernatant differed markedly from that of the medium; a difference corroborated by PCA (Fig. 1A, B). Compared to the culture medium, the concentration of 33 metabolites was higher and that of 13 metabolites was lower. Particularly, the culture supernatant contained an extremely high LA concentration. To interpret the biological implications of the metabolites secreted by ADSCs, we performed MSEA on metabolites detected at higher concentration than in the culture medium and found that various metabolic pathways were activated, especially involving the Warburg effect (Fig. 1C). The Warburg effect is a phenomenon

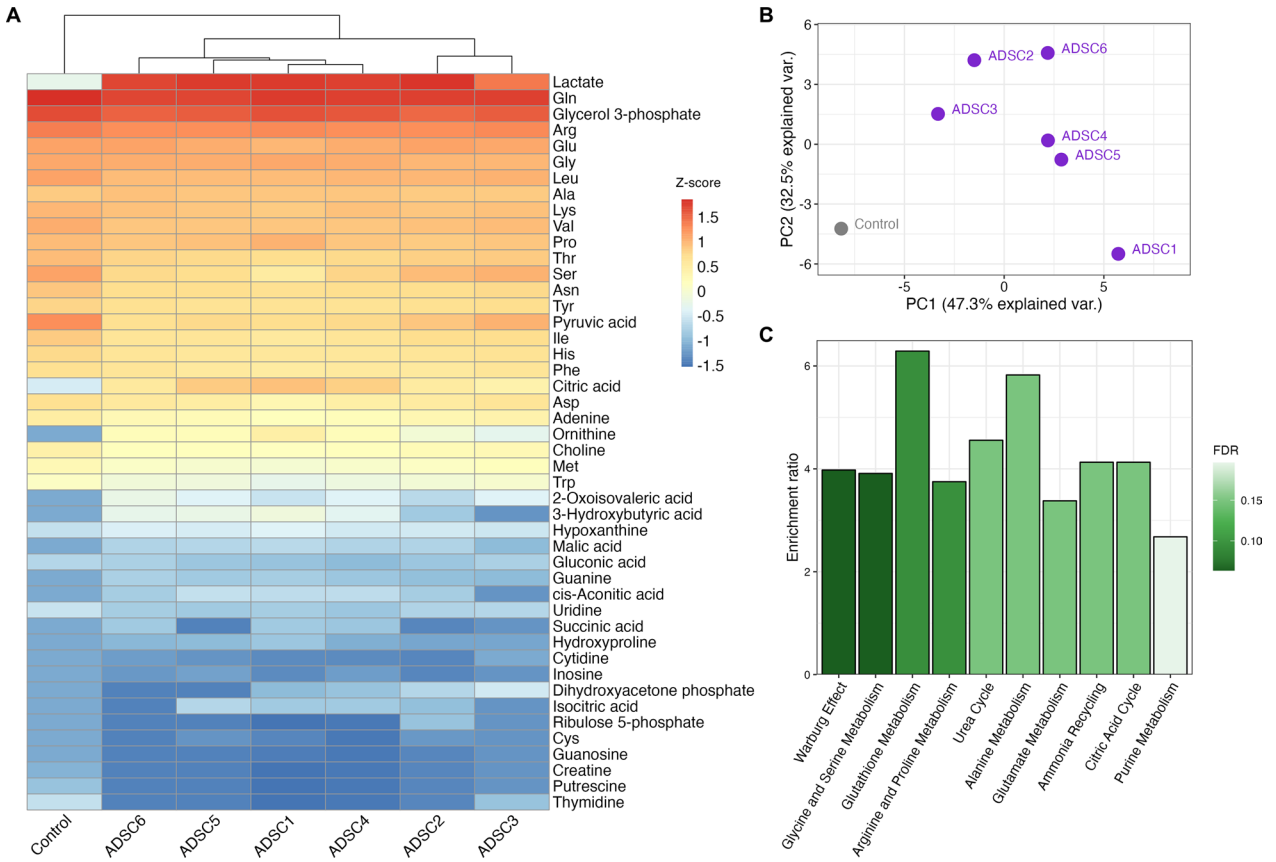

Fig. 1 Metabolomic analysis showing that ADSCs secrete large amounts of lactate. **A** Heatmap from metabolomic analysis results. The color corresponds to a Z-score calculated from the log2-transformed (adding 1 as pseudocount) concentration (in red: high concentration, in blue: low concentration). **B** Principal component analysis (PCA) of the data acquired by metabolomic analysis. **C** The bar plot from the MSEA result. The y-axis and the color of bar represent the enrichment ratio and false discovery rate (FDR), respectively

whereby glycolysis is enhanced, and the production of LA is increased [38].

Effect of lactate and conditioned ADSC medium on M1-like macrophages

In diseases including OA, ADSCs have been reported to suppress the pro-inflammatory response of M1-like macrophages [39, 40]. Moreover, some research groups have indicated that LA induces macrophage polarization toward an M2 phenotype [41]. Therefore, in vitro experiments were carried out using human monocytic THP-1 cells to test whether ADSC-derived LA could induce anti-inflammatory effects. Previous reports showed that THP-1 cells differentiated into M0 macrophages and polarized toward M1-like macrophages using PMA and LPS, respectively; we confirmed that these treatments successfully induced differentiation/polarization by detecting CD11b (a pan-macrophage marker) and CD80 (a M1-like macrophage marker) expression using flow cytometry (Fig. S2A–D) [42, 43]. We next conducted an Annexin V assay to assess the effect of LA on macrophages; no change in the percentage of apoptotic cells was observed up to 15 mM (Fig. 2A, B). Therefore, we used 15 mM LA in subsequent experiments.

Next, we performed a transcriptomic analysis to investigate how the conditioned ADSC medium and LA affect gene expression in macrophages. PCA revealed a distinct difference among the controls (medium only), CM prepared from commercially available ADSCs, and 15 mM LA-treated cells (Fig. 3A). Compared to the controls, 2814 and 3621 genes were significantly upregulated by CM and LA treatment, respectively (Fig. 3B–D). Conversely, 3,070 genes in CM-treated cells and 3,561 genes in LA-treated cells were significantly downregulated (Fig. 3B, C, E). Next, we performed GO analysis for co-upregulated and co-downregulated genes (877 and 983, respectively) in CM and LA as shown in Fig. 3F, G. Differentially expressed genes were highly clustered some ontologies, e.g., "wound healing" is associated with an anti-inflammatory property of macrophages [44]. These results suggested that both the CM and LA dramatically alter the properties of M1-like macrophages.

Lactate has an anti-inflammatory effect but probably does not induce M2 polarization

Considering previous reports describing that ADSCs polarize macrophages from an M1 to an M2 phenotype, we next examined whether this function is mediated by secreted LA [26, 45]. Differential expression analysis of our RNA-seq data revealed a significantly increased expression of M2-like macrophage markers like *CD209* and *VEGFA* in CM- and LA-treated macrophages. On the contrary, the expression levels of *TNF*, which codes TNF-α (a typical inflammatory cytokine) and *PTGS2*, which encodes cyclooxygenase 2, an enzyme important in inflammatory responses, were significantly decreased by CM and LA treatment (Fig. 4A, B) [34, 46–50]. In addition, CM treatment significantly suppressed the expression of inducible nitric oxide synthase (iNOS coded by *NOS2*), a major functional marker of M1-like macrophages, and increased that of CD163, a representative cell surface marker of M2-like macrophages, at both the gene and protein levels (Fig. 4A–G). Consistent with these results, CM harvested from in-house ADSCs also secreted comparable LA concentration to commercially available ADSCs and showed similar gene expression profiles (Figs. S1, S3A–D). The expression of arginase-1 (coded by *ARG1*), which is used as a representative

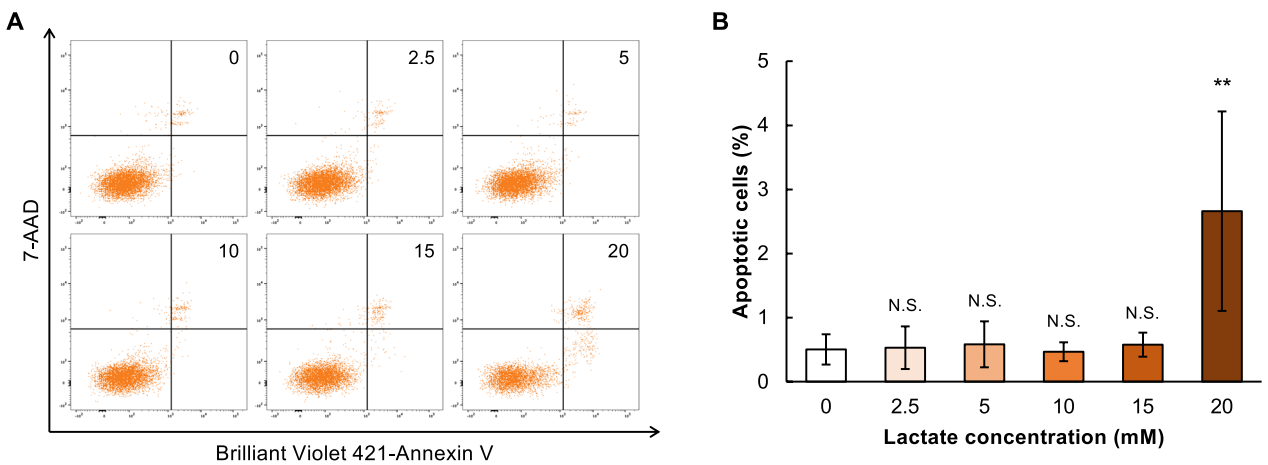

Fig. 2 Effects of lactate on macrophage viability. **A** Representative dot plots and **B** percentage of apoptotic cells with lactate treatment ($n = 3$). The numbers in **A** represent the concentration of lactate. $^{**}P < 0.01$. N.S., not significant

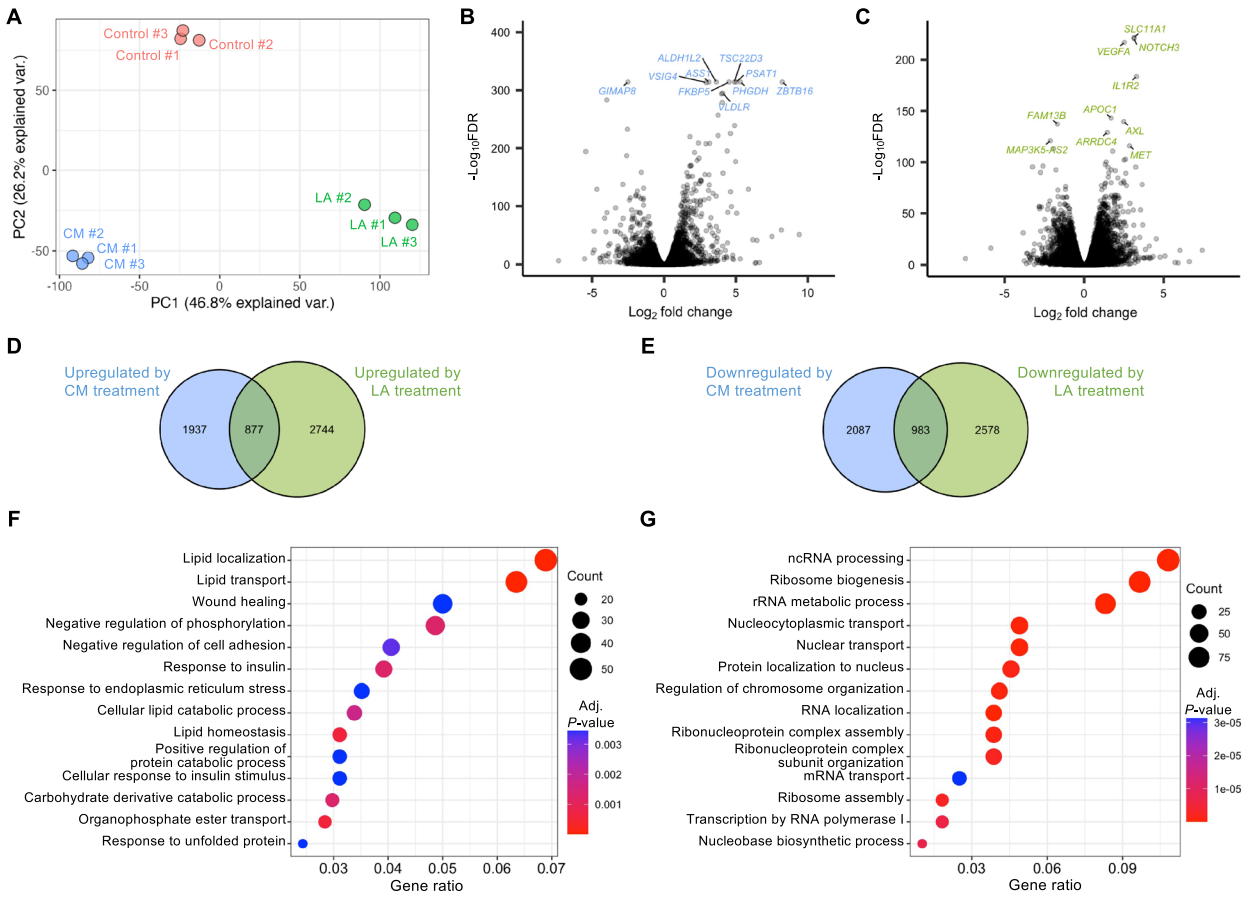

Fig. 3 Conditioned ADSC medium and lactate alter the gene expression profiles of M1-like macrophages. **A** PCA of RNA-seq data. **B** and **C** Volcano plots showing 10 most differentially expressed genes between **B** control (Control) and conditioned medium-treated cells (CM) or **C** control and lactate-treated cells (LA). The abscissa and ordinate represent $\log_2$ (fold change) and $-\log_{10}$(FDR), respectively. **D** and **E** Venn diagrams illustrating the overlap of genes significantly **D** upregulated or **E** downregulated by conditioned medium or lactate treatment. **F** and **G** Dot plots showing the result of GO analysis associated with **F** co-upregulated or **G** co-downregulated genes

functional marker for M2-like macrophages, was undetectable at mRNA (Fig. 4B) and protein (Additional File 3) levels in all samples.

Previous reports have shown that apoptotic cells regulate the function of surrounding cells via metabolites, and we tested the anti-inflammatory effect of apoptotic ADSCs on M1-like macrophages [35, 36]. In this study, the p53-MDM2 inhibitor nutlin-3 was used to induce apoptosis [51, 52]. The percentage of Annexin V^+ 7-AAD^- apoptotic cells was significantly increased at 24 and 48 h after applying 10 μM and 20 μM of nutlin-3 (Fig. S4A, B). Furthermore, trypan blue exclusion assay showed that 20 μM nutlin-3 significantly induced a decrease in cell viability at both 24 and 48 h time points (Figs. S4C, D). Nutlin-3-induced apoptotic ADSCs secreted comparable LA concentration compared to control cells, and no significant differences were observed in the effects of culture supernatant on the gene expression in M1-like macrophages (Fig. S3E–J).

Despite the reduced expression of pro-inflammatory factors, as noted above, no significant changes in the key marker expression were observed in the LA-treated cells; rather, the protein level of CD80 (a major M1-like macrophage markers) was upregulated (Fig. 4A–G). These results suggested that LA has an anti-inflammatory effect but may not be mediated by polarization from M1- to M2-like macrophages.

Lactate induces histone acetylation rather than NF-κB signaling suppression

We then examined how LA suppresses the pro-inflammatory effect of M1-like macrophages. Macrophage stimulation by pathogens and/or cytokines like LPS and INF-γ activates NF-κB signaling, a master regulator

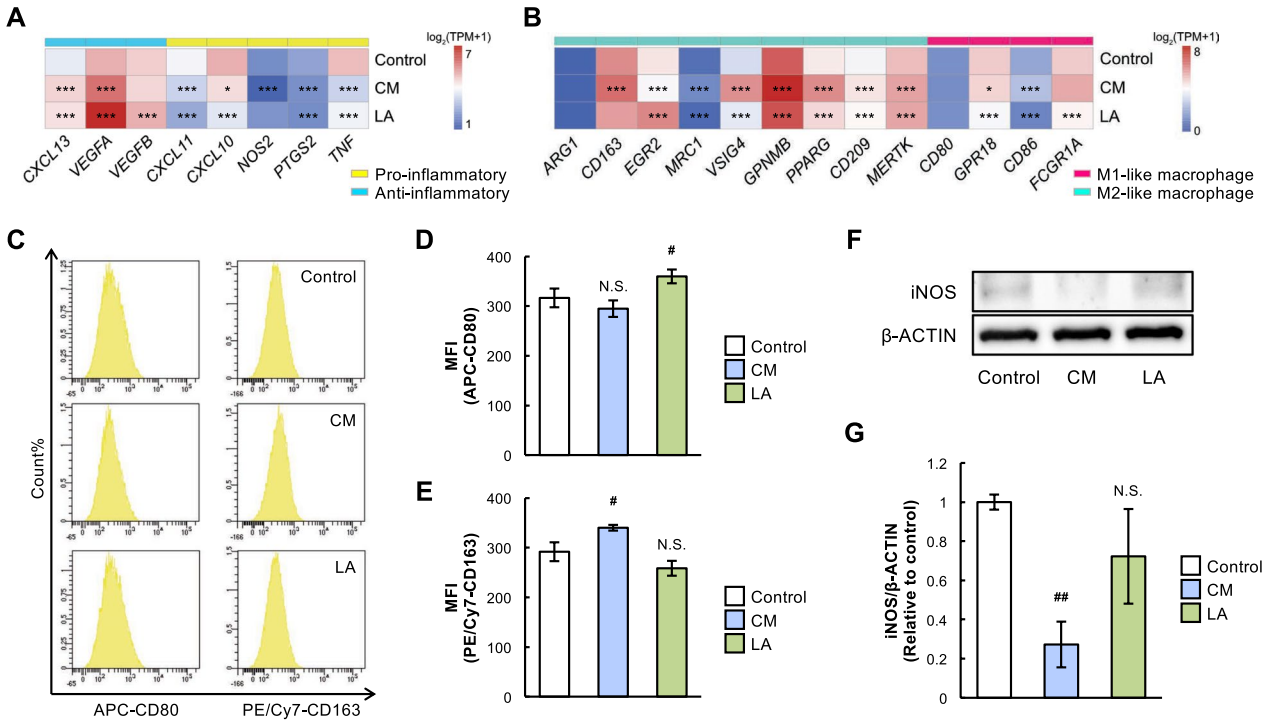

Fig. 4 Both conditioned medium and lactate suppress pro-inflammatory responses of M1-like macrophages. **A** and **B** Heatmap showing mRNA expression levels of **A** inflammation-related factors and **B** representative markers of M1- and M2-like macrophages. Red and blue represent high and low expression ($\log_2$(TPM + 1)). **C**–**E** **C** Representative histograms and mean fluorescence intensity (MFI) of **D** CD80 and **E** CD163 ($n = 3$). **F** and **G** **F** Representative images of immunoblotting and **G** protein levels of iNOS ($n = 3$). β-ACTIN was used as a loading control. *FDR < 0.05, ***FDR < 0.001, $^{\#}P < 0.05$, $^{\#\#}P < 0.01$. N.S., not significant

of inflammatory responses, followed by activating the transcription of genes encoding pro-inflammatory cytokines [53]. Therefore, we hypothesized that LA might suppress NF-κB signaling. As already known, LPS treatment of M0 macrophages induced nuclear translocation of NF-κB p65 subunit and degradation of cytoplasmic IκBα in a time-dependent manner (Fig. S5A) [54]. However, no remarkable difference was observed in p65 or IκB phosphorylation levels after the LA treatment (Fig. S5B). In other words, LA had little effect on the NF-κB signaling activity, at least under the conditions of the present experiment.

A new study recently reported that LA suppresses the inflammatory response of M1-like macrophages, which showed that LA does not suppress NF-κB signaling but rather exerts its anti-inflammatory effects through transcriptional regulation via H3K27 acetylation [34]. GO analysis of our RNA-seq data suggested that both LA and CM treatment altered gene transcription (Figs. 5A, B, S6A, B). Interestingly, consistent with these results, LA treatment for 6 h increased H3K27ac expression (Fig. 5D), indicating that the anti-inflammatory effect of LA may be associated with transcription changes.

Inhibition of a lactate transporter cancels the effect of the conditioned medium

In our experimental conditions, CM and LA had similar effects on M1-like macrophages in terms of suppressing inflammatory profiles. However, the presence of other compounds than LA in the CM (Fig. 1A) might influence the observed results. Therefore, we examined whether the effect of CM could be inhibited by pharmacologically inhibiting LA uptake in M1-like macrophages. Since LA influx and efflux in macrophages are mainly carried out by monocarboxylate transporter 1 (MCT1) and MCT4, respectively, we used the selective MCT1 inhibitor 7ACC2 [55–57]. Previous reports have shown that 7ACC2 specifically inhibits LA uptake in cells expressing both MCT1 and MCT4; using RNA-seq, we confirmed that THP-1 cells highly express *SLC16A1* (MCT1) and *SLC16A4* (MCT4) compared to other MCTs (*SLC16A7* and *SLC16A8*, coding MCT2 and MCT3, respectively; Fig. 6A) [57]. A cell viability assay showed no significant change in survival rates at 24 h after 7ACC2 treatment within the 1–20 μM range (Fig. 6B). Intracellular LA levels significantly decreased when LA was added in the presence of the inhibitor, indicating that the LA uptake was inhibited by 7ACC2 (Fig. 6C). As expected,

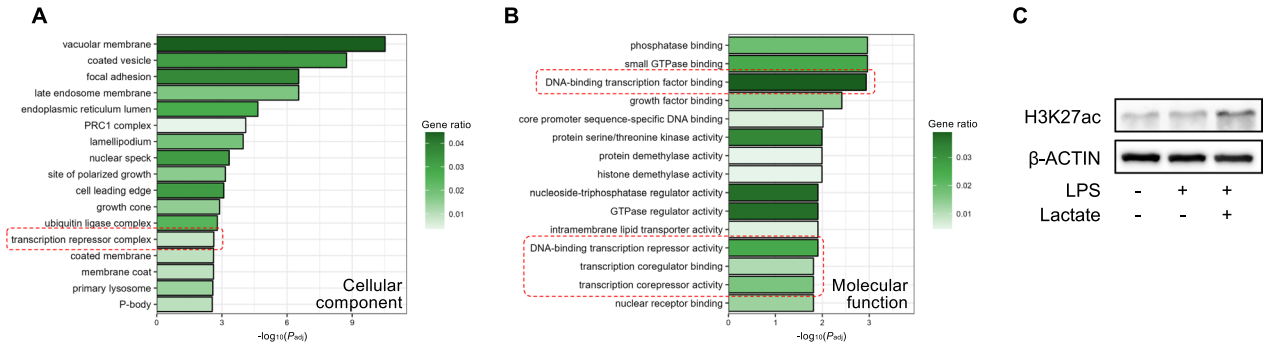

Fig. 5 Lactate may alter transcription via histone acetylation. **A** and **B** GO analysis was performed using genes whose expression was upregulated by lactate treatment. The results of GO analysis related to **A** cellular component and **B** molecular function are represented by bar plots. **C** Representative images of immunoblotting. β-ACTIN was used as a loading control

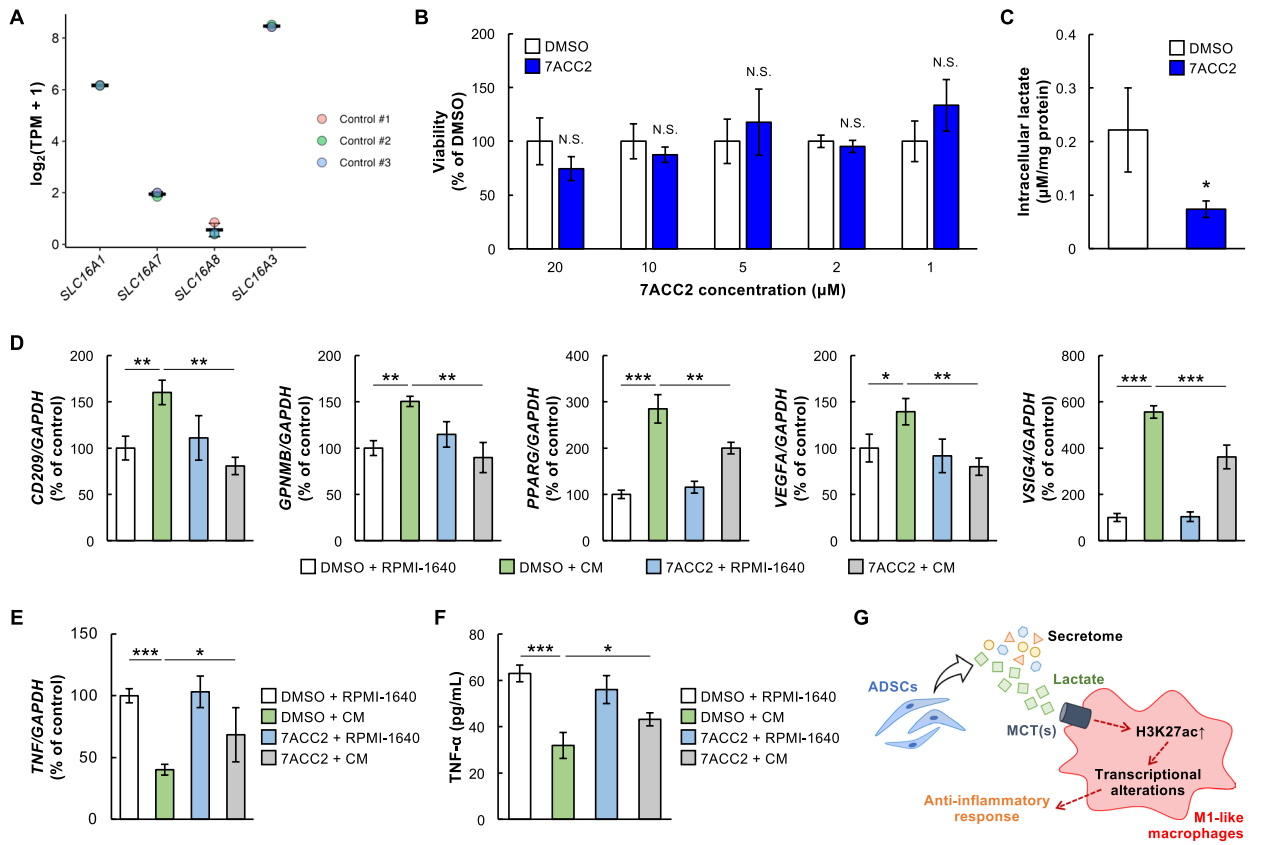

Fig. 6 Inhibiting lactate uptake prevents M2-like macrophage polarization by conditioned ADSC medium. **A** MCT1–4 expression in M1-like macrophages measured by RNA-seq (Control #1–#3) ($n=3$). **B** Cell viability of macrophages treated with 7ACC2 at 1–20 μM ($n=3$). **C** Intracellular lactate concentration ($n=3$). **D** Gene expressions of representative M2-like macrophage markers ($n=3$). **E** and **F** **E** *TNF* expression and **F** the concentration of TNF-α in the medium ($n=4$). **G** Summary of this study. Lactate secreted by ADSCs exerts anti-inflammatory effects, which is induced by lactate taken up by M1-like macrophages via MCT(s), probably by regulating gene transcription through histone acetylation. $^{*}P<0.05$, $^{**}P<0.01$, $^{***}P<0.001$. N.S., not significant

the expression of *CD209*, *GPNMB*, *PPARG*, *VEGFA*, and *VSIG4*, which were increased by CM treatment, significantly decreased with 7ACC2 (Fig. 6D). In addition, *TNF* mRNA expression and TNF-α production decreased by CM stimulation; an effect inhibited by 7ACC2 administration (Fig. 6E, F).

Finally, to evaluate the therapeutic effect of LA in CM, in vivo experiments were performed using a mouse

model of OA, a representative inflammatory disease. We employed the widely used type VII collagenase-induced OA model (Fig. S7A) [58, 59]. This model induces OA by deteriorating tendons and ligaments rather than directly degrading articular cartilage [60]. Histological analysis showed that articular cartilage was significantly reduced through collagenase treatment (Fig. S7B). Although CM partially rescued collagenase-induced cartilage lesions, the application of 7ACC2 tended to diminish the effect of CM, albeit not significantly (Fig. S7C). In line with previous reports, immunofluorescence staining showed an increased number of $CD14^+$ M1-like macrophages with OA onset, while that of $CD163^+$ M2-like macrophages did not change (Fig. S7D, E) [61, 62]. In addition, there was no change in the number of M1- or M2-like macrophages between CM and CM + 7ACC2 (Fig. S7F, G), consistent with our in vitro results showing that LA did not affect macrophage polarization (Fig. 4) and another previous report [34].

Overall, LA secreted from ADSCs is incorporated into M1-like macrophages via MCTs (partially MCT1) and exhibits anti-inflammatory effects through transcriptional regulation via histone acetylation (Fig. 6G).

Discussion

In this study, we performed a comprehensive metabolomic analysis on culture supernatants of ADSCs isolated from humans; although some studies have performed metabolomic analysis on ADSCs' secretion products, they were performed on mouse or rat ADSCs [63, 64]; to the best of our knowledge, this is the first study to reveal the detailed metabolite profiles of human ADSCs.

Despite the existence of previous reports on the LA secreted from ADSCs, most are related to the energy metabolism of ADSCs themselves; in other words, LA is considered as a "waste" produced by altered metabolic systems, and the functional role of secreted LA was not clear, thus far [64–66]. In this study, LA secreted by ADSCs suppresses the pro-inflammatory activity of M1-like macrophages. Since inflammatory responses are mainly elicited by M1-like macrophages, strategies to suppress the pro-inflammatory cytokine production would be effective against inflammatory diseases; in this regard, enhancing LA secretion from ADSCs may be clinically beneficial. LA has been shown to be secreted in large amounts in previous metabolomic analysis of mouse ADSCs [64], suggesting that this might be a common phenomenon across species.

Previous studies revealed that LA production from ADSCs increased under hypoxia [65–67]. Interestingly, oxygen levels in the normal knee joint are maintained in hypoxic conditions but increase with OA progression [68]. Treatment with ADSCs has weak effects in patients with severe OA, possibly by suppressing LA secretion from ADSCs due to oxygen concentration changes within the knee joint [69]. Further studies are needed to determine whether LA contributes to the therapeutic effects against various inflammatory diseases (e.g., arthritis, inflammatory bowel disease and sepsis) by in vivo experiments. Referring to OA, where ADSCs are frequently used during therapy, the conditioned ADSC medium alleviated OA symptoms, and it would be worthwhile to investigate whether LA also contributes to the therapeutic effect of ADSCs in vivo [21, 70, 71]. However, LA may yield positive and negative effects on OA. For example, LA is expected to exert its therapeutic effects by suppressing the expression of ADAMTS5, a typical extracellular matrix-degrading protease, by increasing the expression of COL2A1, a significant component of the articular cartilage, or by suppressing the migration and IL-6 production of synovial macrophages [72, 73]. Conversely, the acidic pH caused by lactic acid may exacerbate symptoms by inhibiting chondrocyte proliferation and matrix synthesis and by promoting IL-6 production from synovial fibroblasts [72, 73]. In this study, the therapeutic effect of LA on OA was investigated using a collagenase-induced mice model, with LA uptake blocked using 7ACC2. At least under the conditions of this study, histological analysis showed that 7ACC2 treatment slightly impaired the reduction of cartilage loss by CM (Fig. S7C). Although M1-like macrophages are reportedly accumulated in collagenase-induced OA, 7ACC2 could not completely cancel the therapeutic effect of CM [74]. This might be because (1) 7ACC2 administered to the knee joint affects not only macrophages but also other cell types such as chondrocytes and synoviocytes and (2) ADSCs secrete various cytokines and EVs in addition to LA, which may also contribute to their therapeutic effect [22, 23]. Therefore, alternative methods (e.g., use of macrophage-specific MCT1-deficient mice and administration of ADSCs with suppressed LA production) to accurately validate the anti-inflammatory effects of LA in vivo need to be explored.

There are several reports on the effects of LA on monocytes and/or macrophages, with tumor cell-derived LA inducing M2 polarization of tumor-associated macrophages and bone marrow-derived MSC-derived LA affecting the differentiation of monocytes to dendritic cells [75, 76]. Further, activation of NF-κB signaling is important for macrophage activation; however, whether LA affects the NF-κB signaling is controversial. For example, Samuvel et al. [77] reported that LA activates NF-κB pathway by boosting TLR4 signaling. On the contrary, Yang et al. and other research groups indicated that LA suppresses pro-inflammatory phenotypes [78–80]. Moreover, Hée et al.

[81] demonstrated that LA does not activate NF-κB signaling under certain conditions. Although the effect of LA on NF-κB pathway is not entirely clear, some studies indicate that LA activates NF-κB signaling in some cell types but not in oxidative cells [81–83]. As previous reports showed that THP-1 cells depend on oxidative phosphorylation for energy production, we do not see any inconsistency between these studies [84, 85] and the present report. It should be noted that a major M2-like macrophage marker ARG1 expression was not observed in this study, possibly because the phenotype of THP-1 cells is biased toward the M1 type, and the expression of *IL10* and *ARG1*, which are characteristic of M2-like macrophages, is relatively low compared to human monocytic U937 cell-derived macrophages [86]. In addition, ARG1 expression varies among species and cell origins, and it is debatable whether ARG1 can be a marker for human M2-like macrophages [87].

Recently, Shi et al. [34] have reported that LA exerts an anti-inflammatory effect through transcriptional alterations via histone acetylation rather than suppressing NF-κB signaling or inducing polarization toward M2-like macrophages. In our experiments, LA increased or decreased the expression of different M1- and M2-like macrophage markers, making it unlikely to induced polarization toward M2-like macrophages. Mechanistically, LA incorporated into macrophages via MCTs is metabolized to citrate as fuel for the TCA cycle, followed by acetylation of histone H3K27, and this histone modification triggers transcriptional program shift toward immunosuppression. They showed that treatment with LPS and LA increased H3K27ac expression in murine macrophages, and trichostatin A, an HDAC inhibitor also promoted H3K27 acetylation. Consistent with their reports, we demonstrated that LA increased H3K27ac expression in human-derived M1-like macrophages (Fig. 5). Furthermore, previous studies have shown that epigenetic changes, especially histone modifications, play an important role in the long-term memory of innate immunity [88, 89]. As discussed by Shi et al. [90] LA-treated macrophages exhibit long-lasting immunosuppressive phenotype. Results of randomized controlled trials have shown that ADSC treatment for OA relieved symptoms even at 12 months postoperatively. These results suggest that ADSCs may, of course, differentiate into chondrocytes and repair tissues. Still, LA secreted from administered ADSCs may cause epigenetic reprogramming of macrophages and induce a long-term immunosuppressive state, resulting in prolonged alleviation of symptoms. Although analyses of detailed molecular mechanisms and experiments using CM have not been performed, the results suggest that high LA concentrations secreted from ADSCs can modify the transcriptional program of M1-like macrophages.

In this study, the recently developed MCT1 inhibitor 7ACC2 was used to block LA uptake. The effect of 7ACC2 varies by cell type, with 7ACC2 effectively inhibiting LA uptake in cells expressing both MCT1 and MCT4. Indeed, transcriptome analysis showed that THP-1 cells highly express both MCT1 and MCT4. However, since LA uptake could not be completely inhibited by 7ACC2, other approaches, such as alternative inhibitors or genetic inhibition, are needed to more accurately examine the impact on macrophages of the LA secreted by ADSCs.

Overall, we demonstrated that ADSCs exert anti-inflammatory effects via LA secretion. As shown in the metabolome analysis, ADSCs secrete other metabolites aside from LA. Medina et al. [36] reported that the combination of multiple metabolites released from apoptotic cells suppress the inflammatory response of myeloid cells. In our study, the percentage of apoptotic macrophages did not change at 24 h of LA exposure. Still, metabolites secreted from apoptotic macrophages present earlier and/or certain metabolite combinations may enhance the observed anti-inflammatory effects. Also, we investigated the effect of apoptotic ADSCs. As no differences in LA secretion capacity or suppression of inflammation were observed in apoptotic ADSCs compared to normal ADSCs under the present conditions, no notable features were observed in apoptotic ADSCs. However, since nutlin-3 mildly induced apoptosis, it would be interesting to investigate the anti-inflammatory effects of apoptotic ADSCs under more severe conditions, such as ultraviolet irradiation.

One limitation of this study is that we cannot rule out the effects of other factors in CM. Since the effect of CM was abolished by 7ACC2 treatment (Fig. 6), LA has an anti-inflammatory effect, but CM and LA have different effects on M1-like macrophages (Fig. 4). As mentioned above, CM is composed of various cytokines and EVs reported to have immunosuppressive effects [22, 23]. That is, the phenotype of M1-like macrophages treated with CM reflects the additive or synergistic effects of these components, which may be why the phenotype differed between CM and LA treatments, as shown in Fig. 4.

Considering the clinical application of this study, the establishment of a new culture method (e.g., developing better culture medium and/or culture dishes) in such a way as to increase the secretory capacity of LA may help to improve the therapeutic outcome of ADSC. Furthermore, LA secretion of cultured ADSCs may be used as a novel biomarker to predict therapeutic effects. Although we have demonstrated a functional role of the metabolite secreted by ADSCs prepared from a limited number

and background of people, it is not clear whether ADSCs from humans with different backgrounds (e.g., race, age, medical history, sex) also secrete large amounts of LA, which should be investigated in the future.

Conclusions

ADSCs derived from healthy individuals showed LA hypersecretion. Further, ADSC-derived LA suppresses the pro-inflammatory effects of M1-like macrophages, presumably through transcriptional modulation via histone acetylation. Accordingly, metabolites, especially LA, could be "new players" with therapeutic potential, aside from cytokines and EVs.

Abbreviations

7-AAD	7-Aminoactinomycin D
ADSC	Adipose-derived stem cell
CE-TOFMS	Capillary electrophoresis time-of-flight mass spectrometry
CM	Conditioned medium
CPM	Counts per million
DMSO	Dimethyl sulfoxide
ELISA	Enzyme-linked immunosorbent assay
EV	Extracellular vesicle
FBS	Fetal bovine serum
FDR	False discovery rate
GO	Gene ontology
HDAC	Histone deacetylase
IL	Interleukin
iNOS	Inducible nitric oxide synthase
iPSC	Induced pluripotent stem cell
LA	Lactate
LPS	Lipopolysaccharide
MCT	Monocarboxylate transporter
MFI	Mean fluorescence intensity
MSC	Mesenchymal stem/stromal cell
MSEA	Metabolite set enrichment analysis
NES	Normalized enrichment score
NF-κB	Nuclear factor-kappa B
OA	Osteoarthritis
PBS	Phosphate buffered saline
PCA	Principal component analysis
PMA	Phorbol 12-myristate 13-acetate
qPCR	Quantitative polymerase chain reaction
RNA-seq	RNA sequencing
RPMI-1640	Roswell Park Memorial Institute 1640
TBP	TATA-binding protein
TBS-T	Tris buffered saline with Tween 20
TNF-α	Tumor necrosis factor-alpha
TPM	Transcripts per million

Supplementary Information

The online version contains supplementary material available at https://doi.org/10.1186/s13287-024-04072-w.

Supplementary file 1.

Supplementary file 2.

Supplementary file 3.

Acknowledgements

The authors would like to thank Ms. Ayane Kuwano (Kanazawa Institute of Technology) for technical assistance with the experiments on the early stages of this work and Ms. Yuka Hiramatsu (Kanazawa Medical University) for her help with the histological analysis. Metabolomic analysis and RNA-seq were performed by Human Metabolome Technologies, Inc. (Yamagata, Japan) and Bioengineering Lab. Co., Ltd. (Kanagawa, Japan), respectively. The supercomputing resource was provided by Human Genome Center, the Institute of Medical Science, the University of Tokyo.

Author contributions

HH, YS, YI, TI and KI contributed to the conceptualization of the work; TH, HH, YI and TI designed the study; TH, TS and YN performed the experiments; TH allocated the in vivo experimental group; IT, HS and YS reviewed methodology; TH, HH, HK, AF, YT, YI, NY and TI interpreted the data; YI, TI, AK, SO and NK supervised the study; TH, HH, YI and TI wrote the manuscript. All authors read and approved the final manuscript.

Funding

This work was supported by JSPS KAKENHI (JP21K16666 and JP22K20726), a Grant for Collaborative Research from Kanazawa Medical University (C2021-3 and C2022-1), grants-in-aid from The Nakatomi Foundation and Shibuya Science Culture and Sports Foundation.

Availability of data and materials

Raw fastq files generated by our RNA-seq were deposited in DNA Data Bank of Japan (accession number: DRA016915). Mass spectrometry data of metabolome analysis was provided as Additional File 2. Other data generated in this study are available from the corresponding authors upon reasonable request.

Declarations

Ethics approval and consent to participate

This study was conducted in accordance with the Declaration of Helsinki and approved by the Kanazawa Medical University Specified Certified Regenerative Medicine Committee, the Institutional Review Board for Genetic Analysis Research according to the following two protocols: (1) Investigation of the regenerative effects of adipose-derived stem cells on various organ failures and gene expression (approval number: G129, date of approval: April 17, 2017); (2) Omics analysis of autologous adipose-derived stem cells for treatment of knee osteoarthritis (approval number: G173, date of approval: June 25, 2021). Informed consent was obtained from all subjects involved in this study.

Consent for publication

Not applicable.

Competing interests

The authors declare that they have no competing interests.

Author details

[1]Medical Research Institute, Kanazawa Medical University, Kahoku, Ishikawa 920-0293, Japan. [2]Department of Pharmacy, Kanazawa Medical University Hospital, Kahoku, Ishikawa 920-0293, Japan. [3]Department of Orthopedic Surgery, Kanazawa Medical University, Kahoku, Ishikawa 920-0293, Japan. [4]Department of Biochemistry I, Kanazawa Medical University, Kahoku, Ishikawa 920-0293, Japan. [5]Genome Biotechnology Laboratory, Kanazawa Institute of Technology, Hakusan, Ishikawa 924-0838, Japan. [6]Advanced Medical Research Center, Faculty of Medicine, University of the Ryukyus, Nakagami, Okinawa 903-0215, Japan. [7]Research Promotion Headquarters, Fujita Health University, Toyoake, Aichi 470-1192, Japan. [8]Department of Plastic and Reconstructive Surgery, Graduate School of Medicine, University of the Ryukyus, Nakagami, Okinawa 903-0215, Japan.

Received: 12 November 2023 Accepted: 20 November 2024
Published online: 18 December 2024

References

1. Clarke G, Harley P, Hubber EL, Manea T, Manuelli L, Read E, et al. Bench to bedside: current advances in regenerative medicine. Curr Opin Cell Biol. 2018;55:59–66.

2. McKinley KL, Longaker MT, Naik S. Emerging frontiers in regenerative medicine. Science. 2023;380:796–8. https://doi.org/10.1126/science.add6492.
3. Hoang DM, Pham PT, Bach TQ, Ngo ATL, Nguyen QT, Phan TTK, et al. Stem cell-based therapy for human diseases. Signal Transduct Target Ther. 2022;7:1–41.
4. Zakrzewski W, Dobrzyński M, Szymonowicz M, Rybak Z. Stem cells: past, present, and future. Stem Cell Res Ther. 2019;10:1–22. https://doi.org/10.1186/s13287-019-1165-5.
5. Kim JY, Nam Y, Rim YA, Ji Hyeon Ju. Review of the current trends in clinical trials involving induced pluripotent stem cells. Stem Cell Rev Rep. 2022;18(1):142–54. https://doi.org/10.1007/s12015-021-10262-3.
6. Ylä-Herttuala S. iPSC-derived cardiomyocytes taken to rescue infarcted heart muscle in coronary heart disease patients. Mol Ther. 2018;26:2077.
7. Ahmed I, Johnston Jr RJ, Singh MS. Pluripotent stem cell therapy for retinal diseases. Ann Transl Med. 2021;9(15):1279–1279. https://doi.org/10.21037/atm-20-4747.
8. Doss MX, Sachinidis A. Current challenges of iPSC-based disease modeling and therapeutic implications. Cells. 2019;8(5):403. https://doi.org/10.3390/cells8050403.
9. Yamanaka S. Pluripotent stem cell-based cell therapy—promise and challenges. Cell Stem Cell. 2020;27:523–31.
10. Orkin SH, Zon LI. Hematopoiesis: an evolving paradigm for stem cell biology. Cell. 2008;132(4):631–44. https://doi.org/10.1016/j.cell.2008.01.025.
11. Cheng H, Zheng Z, Cheng T. New paradigms on hematopoietic stem cell differentiation. Protein Cell. 2020;11:34–44. https://doi.org/10.1007/s13238-019-0633-0.
12. Zhao X, Moore DL. Neural stem cells: developmental mechanisms and disease modeling. Cell Tissue Res. 2018;371(1):1–6. https://doi.org/10.1007/s00441-017-2738-1.
13. Hamilton BK, Copelan EA. Concise review: the role of hematopoietic stem cell transplantation in the treatment of acute myeloid leukemia. Stem Cells. 2012. https://doi.org/10.1002/stem.1140.
14. Kassim AA, Savani BN. Hematopoietic stem cell transplantation for acute myeloid leukemia: a review. Hematol Oncol Stem Cell Ther. 2017;10(4):245–51. https://doi.org/10.1016/j.hemonc.2017.05.021.
15. Ntege EH, Sunami H, Shimizu Y. Advances in regenerative therapy: a review of the literature and future directions. Regen Ther. 2020;14:136–53.
16. Pittenger MF, Discher DE, Péault BM, Phinney DG, Hare JM, Caplan AI. Mesenchymal stem cell perspective: cell biology to clinical progress. NPJ Regen Med. 2019;4:1. https://doi.org/10.1038/s41536-019-0083-6.
17. Ledesma-Martínez E, Mendoza-Núñez VM, Santiago-Osorio E. Mesenchymal stem cells derived from dental pulp: a review. Stem Cells Int. 2016. https://doi.org/10.1155/2016/4709572.
18. Schneider S, Unger M, van Griensven M, Balmayor ER. Adipose-derived mesenchymal stem cells from liposuction and resected fat are feasible sources for regenerative medicine. Eur J Med Res. 2017. https://doi.org/10.1186/s40001-017-0258-9.
19. Si Z, Wang X, Sun C, Kang Y, Xu J, Wang X, et al. Adipose-derived stem cells: sources, potency, and implications for regenerative therapies. Biomed Pharmacother. 2019;114:108765.
20. Gao F, Chiu SM, Motan DAL, Zhang Z, Chen L, Ji HL, et al. Mesenchymal stem cells and immunomodulation: current status and future prospects. Cell Death Dis. 2016;7:e2062.
21. Ceccarelli S, Pontecorvi P, Anastasiadou E, Napoli C, Marchese C. Immunomodulatory effect of adipose-derived stem cells: the cutting edge of clinical application. Front Cell Dev Biol. 2020;8:531513.
22. Ferreira JR, Teixeira GQ, Santos SG, Barbosa MA, Almeida-Porada G, Gonçalves RM. Mesenchymal stromal cell secretome: influencing therapeutic potential by cellular pre-conditioning. Front Immunol. 2018;9:2837. https://doi.org/10.3389/fimmu.2018.02837.
23. Zhao C, Chen J-Y, Peng W-M, Yuan B, Bi Q, Xu Y-J. Exosomes from adipose-derived stem cells promote chondrogenesis and suppress inflammation by upregulating miR-145 and miR-221. Mol Med Rep. 2020. https://doi.org/10.3892/mmr.2020.10982.
24. Heo JS, Choi Y, Kim HO. Adipose-derived mesenchymal stem cells promote M2 macrophage phenotype through exosomes. Stem Cells Int. 2019;2019:1–10. https://doi.org/10.1155/2019/7921760.
25. Liu J, Qiu P, Qin J, Xiaoyu Wu, Wang X, Yang X, Li Bo, Zhang W, Ye K, Peng Z, Xinwu Lu. Allogeneic adipose-derived stem cells promote ischemic muscle repair by inducing M2 macrophage polarization via the HIF-1α/IL-10 pathway. Stem Cells. 2020;38(10):1307–20. https://doi.org/10.1002/stem.3250.
26. Kamada K, Matsushita T, Yamashita T, Matsumoto T, Iwaguro H, Sobajima S, Kuroda R. Attenuation of knee osteoarthritis progression in mice through polarization of M2 macrophages by intra-articular transplantation of non-cultured human adipose-derived regenerative cells. J Clin Med. 2021;10(19):4309. https://doi.org/10.3390/jcm10194309.
27. Guillén MI, Platas J, María D, del Caz P, Mirabet V, Alcaraz MJ. Paracrine anti-inflammatory effects of adipose tissue-derived mesenchymal stem cells in human monocytes. Front Physiol. 2018;9:341918. https://doi.org/10.3389/fphys.2018.00661.
28. Bai X, Li J, Li L, Liu M, Liu Y, Cao M, Tao Ke, Xie S, Dahai Hu. Extracellular vesicles from adipose tissue-derived stem cells affect Notch-miR148a-3p Axis to regulate polarization of macrophages and alleviate sepsis in mice. Front Immunol. 2020. https://doi.org/10.3389/fimmu.2020.01391.
29. Fukuzumi M, Shinomiya H, Shimizu Y, Ohishi K, Utsumi S. Endotoxin-induced enhancement of glucose influx into murine peritoneal macrophages via GLUT1. Infect Immun. 1996;64(1):108–12. https://doi.org/10.1128/iai.64.1.108-112.1996.
30. Freemerman AJ, Johnson AR, Sacks GN, Justin Milner J, Kirk EL, Troester MA, Macintyre AN, Goraksha-Hicks P, Rathmell JC, Makowski L. Metabolic reprogramming of macrophages. J Biol Chem. 2014;289(11):7884–96. https://doi.org/10.1074/jbc.M113.522037.
31. Greenberg MVC, Bourc'his D. The diverse roles of DNA methylation in mammalian development and disease. Nat Rev Mol Cell Biol. 2019;20(10):590–607. https://doi.org/10.1038/s41580-019-0159-6.
32. Bannister AJ, Kouzarides T. Regulation of chromatin by histone modifications. Cell Res. 2011;21:381–95.
33. Noe JT, Rendon BE, Geller AE, Conroy LR, Morrissey SM, Young LEA, et al. Lactate supports a metabolic-epigenetic link in macrophage polarization. Sci Adv. 2021;7:8602.
34. Shi W, Cassmann TJ, Bhagwate AV, Taro Hitosugi WK, Ip E. Lactic acid induces transcriptional repression of macrophage inflammatory response via histone acetylation. Cell Rep. 2024;43(2):113746. https://doi.org/10.1016/j.celrep.2024.113746.
35. Niemann B, Haufs-Brusberg S, Puetz L, Feickert M, Jaeckstein MY, Hoffmann A, Zurkovic J, Heine M, Trautmann E-M, Müller CE, Tönjes A, Schlein C, Jafari A, Eltzschig HK, Gnad T, Blüher M, Krahmer N, Kovacs P, Heeren J, Pfeifer A. Apoptotic brown adipocytes enhance energy expenditure via extracellular inosine. Nature. 2022;609(7926):361–8. https://doi.org/10.1038/s41586-022-05041-0.
36. Medina CB, Mehrotra P, Arandjelovic S, Perry JSA, Guo Y, Morioka S, Barron B, Walk SF, Ghesquière B, Krupnick AS, Lorenz U, Ravichandran KS. Metabolites released from apoptotic cells act as tissue messengers. Nature. 2020;580(7801):130–5. https://doi.org/10.1038/s41586-020-2121-3.
37. Fuku A, Taki Y, Nakamura Y, Kitajima H, Takaki T, Koya T, Tanida I, Nozaki K, Sunami H, Hirata H, Tachi Y, Masauji T, Yamamoto N, Ishigaki Y, Shimodaira S, Shimizu Y, Ichiseki T, Kaneuji A, Osawa S, Kawahara N. Evaluation of the usefulness of human adipose-derived stem cell spheroids formed using SphereRing® and the lethal damage sensitivity to synovial fluid in vitro. Cells. 2022;11(3):337. https://doi.org/10.3390/cells11030337.
38. Liberti MV, Locasale JW. The warburg effect: how does it benefit cancer cells? Trends Biochem Sci. 2016;41(3):211–8. https://doi.org/10.1016/j.tibs.2015.12.001.
39. Chang T-H, Chien-Sheng Wu, Chiou S-H, Chang C-H, Liao H-J. Adipose-derived stem cell exosomes as a novel anti-inflammatory agent and the current therapeutic targets for rheumatoid arthritis. Biomedicines. 2022;10(7):1725. https://doi.org/10.3390/biomedicines10071725.
40. Jia Q, Zhao H, Wang Y, Cen Y, Zhang Z. Mechanisms and applications of adipose-derived stem cell-extracellular vesicles in the inflammation of wound healing. Front Immunol. 2023;14:1214757.
41. Zhou H-C, Yan X-Y, Wen-wen Yu, Liang X-Q, Xiao-yan Du, Liu Z-C, Long J-P, Zhao G-H, Liu H-B. Lactic acid in macrophage polarization: the significant role in inflammation and cancer. Int Rev Immunol. 2021;41(1):4–18. https://doi.org/10.1080/08830185.2021.1955876.
42. Lin F, Yin H-B, Li X-Y, Zhu G-M, He W-Y, Gou X. Bladder cancer cell-secreted exosomal miR-21 activates the PI3K/AKT pathway in macrophages to promote cancer progression. Int J Oncol. 2019. https://doi.org/10.3892/ijo.2019.4933.

43. Deng Y, Govers C, ter Beest E, van Dijk AJ, Hettinga K, Wichers HJ. A THP-1 cell line-based exploration of immune responses toward heat-treated BLG. Front Nutr. 2021;7:612397.
44. Krzyszczyk P, Schloss R, Palmer A, Berthiaume F. The role of macrophages in acute and chronic wound healing and interventions to promote pro-wound healing phenotypes. Front Physiol. 2018;9:419. https://doi.org/10.3389/fphys.2018.00419.
45. Manferdini C, Paolella F, Gabusi E, Gambari L, Piacentini A, Filardo G, et al. Adipose stromal cells mediated switching of the pro-inflammatory profile of M1-like macrophages is facilitated by PGE2: in vitro evaluation. Osteoarthr Cartil. 2017;25:1161–71.
46. Yao Y, Xu XH, Jin L. Macrophage polarization in physiological and pathological pregnancy. Front Immunol. 2019;10:434399.
47. Zhou L, Zhuo H, Ouyang H, Liu Y, Yuan F, Sun L, et al. Glycoprotein non-metastatic melanoma protein b (Gpnmb) is highly expressed in macrophages of acute injured kidney and promotes M2 macrophages polarization. Cell Immunol. 2017;316:53–60.
48. Yan Wang Yu, Zhang JL, Li C, Zhao R, Shen C, Liu W, Rong J, Wang Z, Ge J, Shi B. Hypoxia induces M2 macrophages to express VSIG4 and mediate cardiac fibrosis after myocardial infarction. Theranostics. 2023;13(7):2192–209. https://doi.org/10.7150/thno.78736.
49. Zizzo G, Hilliard BA, Monestier M, Cohen PL. Efficient clearance of early apoptotic cells by human macrophages requires M2c polarization and MerTK induction. J Immunol. 2012;189:3508–20.
50. Xie Y, Chen Z, Zhong Q, Zheng Z, Chen Y, Shangguan W, Zhang Y, Yang J, Zhu D, Xie W. M2 macrophages secrete CXCL13 to promote renal cell carcinoma migration, invasion, and EMT. Cancer Cell Int. 2021;21:1. https://doi.org/10.1186/s12935-021-02381-1.
51. Vassilev LT, Vu BT, Graves B, Carvajal D, Podlaski F, Filipovic Z, et al. In vivo activation of the p53 pathway by small-molecule antagonists of MDM2. Science. 2004;303:844–8.
52. Vassilev LT. Small-molecule antagonists of p53-MDM2 binding: research tools and potential therapeutics. Cell Cycle. 2014;3(4):417–9. https://doi.org/10.4161/cc.3.4.801.
53. Dorrington MG, Fraser IDC. NF-κB signaling in macrophages: dynamics, crosstalk, and signal integration. Front Immunol. 2019;10:443978.
54. Liu T, Zhang L, Joo D, Sun SC. NF-κB signaling in inflammation. Signal Transduct Target Ther. 2017;2:1.
55. Jha MK, Passero JV, Rawat A, Ament XH, Yang F, Vidensky S, et al. Macrophage monocarboxylate transporter 1 promotes peripheral nerve regeneration after injury in mice. J Clin Invest. 2021. https://doi.org/10.1172/JCI141964.
56. Tan Z, Xie N, Banerjee S, Cui H, Fu M, Thannickal VJ, et al. The monocarboxylate transporter 4 is required for glycolytic reprogramming and inflammatory response in macrophages. J Biol Chem. 2015;290:46.
57. Draoui N, Schicke O, Seront E, Bouzin C, Sonveaux P, Riant O, et al. Antitumor activity of 7-aminocarboxycoumarin derivatives, a new class of potent inhibitors of lactate influx but not efflux. Mol Cancer Ther. 2014. https://doi.org/10.1158/1535-7163.MCT-13-0653.
58. Maumus M, Roussignol G, Toupet K, Penarier G, Bentz I, Teixeira S, et al. Utility of a mouse model of osteoarthritis to demonstrate cartilage protection by IFNγ-primed equine mesenchymal stem cells. Front Immunol. 2016;7:218572.
59. Lee MC, Saleh R, Achuthan A, Fleetwood AJ, Förster I, Hamilton JA, et al. CCL17 blockade as a therapy for osteoarthritis pain and disease. Arthr Res Ther. 2018;20:1–10. https://doi.org/10.1186/s13075-018-1560-9.
60. Alves-Simões M. Rodent models of knee osteoarthritis for pain research. Osteoarthr Cartil. 2022;30:802–14.
61. Boneva B, Ralchev N, Ganova P, Tchorbanov A, Mihaylova N. Collagenase-induced mouse model of osteoarthritis—a thorough flow cytometry analysis. Life. 2022;12:1938.
62. Lv Z, Xu X, Sun Z, Yang YX, Guo H, Li J, et al. TRPV1 alleviates osteoarthritis by inhibiting M1 macrophage polarization via Ca_{2+}/CaMKII/Nrf2 signaling pathway. Cell Death Dis. 2021;12:6.
63. Yang C, Zhang J, Wu T, Zhao K, Wu X, Shi J, et al. Multi-omics analysis to examine gene expression and metabolites from multisite adipose-derived mesenchymal stem cells. Front Genet. 2021;12:627347.
64. Lefevre C, Panthu B, Naville D, Guibert S, Pinteur C, Elena-Herrmann B, Vidal H, Rautureau GJP, Mey A. Metabolic phenotyping of adipose-derived stem cells reveals a unique signature and intrinsic differences between fat pads. Stem Cells Int. 2019;2019:1–16. https://doi.org/10.1155/2019/9323864.
65. Mischen BT, Follmar KE, Moyer KE, Buehrer B, Olbrich KC, Scott Levin L, Klitzman B, Erdmann D. Metabolic and functional characterization of human adipose-derived stem cells in tissue engineering? Plast Reconstr Surg. 2008;122(3):725–38. https://doi.org/10.1097/PRS.0b013e318180ec9f.
66. Park HS, Kim JH, Sun BK, Song SU, Suh W, Sung J-H. Hypoxia induces glucose uptake and metabolism of adipose-derived stem cells. Mol Med Rep. 2016;14(5):4706–14. https://doi.org/10.3892/mmr.2016.5796.
67. Rhijn M-V, Mensah FKF, Korevaar SS, Leijs MJ, van Osch GJVM, IJzermans NMJ, et al. Effects of hypoxia on the immunomodulatory properties of adipose tissue-derived mesenchymal stem cells. Front Immunol. 2013. https://doi.org/10.3389/fimmu.2013.00203.
68. Okada K, Mori D, Makii Y, Nakamoto H, Murahashi Y, Yano F, et al. Hypoxia-inducible factor-1 alpha maintains mouse articular cartilage through suppression of NF-κB signaling. Sci Rep. 2020;10:1.
69. Yokota N, Hattori M, Ohtsuru T, Otsuji M, Lyman S, Shimomura K, et al. Comparative clinical outcomes after intra-articular injection with adipose-derived cultured stem cells or noncultured stromal vascular fraction for the treatment of knee osteoarthritis. Am J Sports Med. 2019;47:2577–83.
70. Cheng JH, Hsu CC, Hsu SL, Chou WY, Wu YN, Kuo CEA, et al. Adipose-derived mesenchymal stem cells-conditioned medium modulates the expression of inflammation induced bone morphogenetic protein-2, -5 and -6 as well as compared with shockwave therapy on rat knee osteoarthritis. Biomedicines. 2021;9:1399.
71. Amodeo G, Niada S, Moschetti G, Franchi S, Savadori P, Brini AT, et al. Secretome of human adipose-derived mesenchymal stem cell relieves pain and neuroinflammation independently of the route of administration in experimental osteoarthritis. Brain Behav Immun. 2021;94:29–40.
72. Zhang X, Wu Y, Pan Z, Sun H, Wang J, Yu D, et al. The effects of lactate and acid on articular chondrocytes function: implications for polymeric cartilage scaffold design. Acta Biomater. 2016;42:329–40.
73. Pucino V, Nefla M, Gauthier V, Alsaleh G, Clayton SA, Marshall J, et al. Differential effect of lactate on synovial fibroblast and macrophage effector functions. Front Immunol. 2023;14:1183825.
74. Zhu X, Lee CW, Xu H, Wang YF, Yung PSH, Jiang Y, et al. Phenotypic alteration of macrophages during osteoarthritis: a systematic review. Arthritis Res Ther. 2021;23:1–13. https://doi.org/10.1186/s13075-021-02457-3.
75. Selleri S, Bifsha P, Civini S, Pacelli C, Dieng MM, Lemieux W, Jin P, Bazin R, Patey N, Marincola FM, Moldovan F, Zaouter C, Trudeau L-E, Benabdhalla B, Louis I, Beauséjour C, Stroncek D, Le Deist F, Haddad E. Human mesenchymal stromal cell-secreted lactate induces M2-macrophage differentiation by metabolic reprogramming. Oncotarget. 2016;7(21):30193–210. https://doi.org/10.18632/oncotarget.8623.
76. Colegio OR, Chu N-Q, Szabo AL, Chu T, Rhebergen AM, Jairam V, Cyrus N, Brokowski CE, Eisenbarth SC, Phillips GM, Cline GW, Phillips AJ, Medzhitov R. Functional polarization of tumour-associated macrophages by tumour-derived lactic acid. Nature. 2014;513(7519):559–63. https://doi.org/10.1038/nature13490.
77. Samuvel DJ, Sundararaj KP, Nareika A, Lopes-Virella MF, Huang Y. Lactate boosts TLR4 signaling and NF-κB pathway-mediated gene transcription in macrophages via monocarboxylate transporters and MD-2 up-regulation. J Immunol. 2009;182(4):2476–84. https://doi.org/10.4049/jimmunol.0802059.
78. Yang K, Xu J, Fan M, Tu F, Wang X, Ha T, et al. Lactate suppresses macrophage pro-inflammatory response to LPS stimulation by inhibition of YAP and NF-κB activation via GPR81-mediated signaling. Front Immunol. 2020;11:587913.
79. Zhou HC, Yu WW, Yan XY, Liang XQ, Ma XF, Long JP, et al. Lactate-driven macrophage polarization in the inflammatory microenvironment alleviates intestinal inflammation. Front Immunol. 2022;13:1013686.
80. Stone SC, Rossetti RAM, Alvarez KLF, Carvalho JP, Margarido PFR, Baracat EC, Tacla M, Boccardo E, Yokochi K, Lorenzi NP, Lepique AP. Lactate secreted by cervical cancer cells modulates macrophage phenotype. J Leukoc Biol. 2019;105(5):1041–54. https://doi.org/10.1002/JLB.3A0718-274RR.
81. Van Hée VF, Pérez-Escuredo J, Cacace A, Copetti T, Sonveaux P. Lactate does not activate NF-κB in oxidative tumor cells. Front Pharmacol. 2015. https://doi.org/10.3389/fphar.2015.00228.

82. Végran F, Boidot R, Michiels C, Sonveaux P, Feron O. Lactate influx through the endothelial cell monocarboxylate transporter MCT1 supports an NF-kB, IL-8 pathway that drives tumor angiogenesis. Cancer Res. 2011. https://doi.org/10.1158/0008-5472.CAN-10-2828.
83. Miller AM, Nolan MJ, Choi J, Koga T, Shen X, Yue BYJT, et al. Lactate treatment causes NF-κB activation and CD44 shedding in cultured trabecular meshwork cells. Invest Ophthalmol Vis Sci. 2007;48:1615–21.
84. Suganuma K, Miwa H, Imai N, Shikami M, Gotou M, Goto M, et al. Energy metabolism of leukemia cells: glycolysis versus oxidative phosphorylation. Leuk Lymphoma. 2010;51:2112–9.
85. Griessinger E, Pereira-Martins D, Nebout M, Bosc C, Saland E, Boet E, et al. Oxidative phosphorylation fueled by fatty acid oxidation sensitizes leukemic stem cells to cold. Cancer Res. 2023. https://doi.org/10.1158/0008-5472.CAN-23-1006.
86. Nascimento CR, Rodrigues Fernandes NA, Gonzalez Maldonado LA, Rossa JC. Comparison of monocytic cell lines U937 and THP-1 as macrophage models for in vitro studies. Biochem Biophys Rep. 2022;32:101383.
87. Thomas AC, Mattila JT. "Of Mice and Men": arginine metabolism in macrophages. Front Immunol. 2014. https://doi.org/10.3389/fimmu.2014.00479.
88. Chen S, Yang J, Wei Y, Wei X. Epigenetic regulation of macrophages: from homeostasis maintenance to host defense. Cell Mol Immunol. 2019;17:1.
89. Netea MG, Domínguez-Andrés J, Barreiro LB, Chavakis T, Divangahi M, Fuchs E, Joosten LAB, van der Meer JWM, Mhlanga MM, Mulder WJM, Riksen NP, Schlitzer A, Schultze JL, Benn CS, Sun JC, Xavier RJ, Latz E. Defining trained immunity and its role in health and disease. Nat Rev Immunol. 2020;20(6):375–88. https://doi.org/10.1038/s41577-020-0285-6.
90. Issa MR, Naja AS, Bouji NZ, Sagherian BH. The role of adipose-derived mesenchymal stem cells in knee osteoarthritis: a meta-analysis of randomized controlled trials. Ther Adv Musculoskelet Dis. 2022. https://doi.org/10.1177/1759720X221146005.

Publisher's Note